Fracture Behaviour of Cracked Functionally Graded Piezoelectric Materials (FGPMs)

Z. Yan, L. Y. Jiang
Department of Mechanical & Materials Engineering
The University of Western Ontario
London, Ontario, Canada

1. Introduction

Piezoelectric materials are widely used as sensors, transducers and actuators because of their excellent electromechanical coupling effect. Due to the advantages of traditional functionally graded materials (FGMs) in reducing residual and thermal stresses [1-2], the concept of FGMs has been introduced into piezoelectric materials. These kinds of new materials are called functionally graded piezoelectric materials (FGPMs), which possess continuous variation in composition and properties. The application of new FGPMs in electromechanical devices is expected to have advantages over the traditionally used homogeneous piezoelectric materials in meeting high demands for their lifetime and reliability. For example, the usage of FGPMs replacing layered piezoelectric components in electromechanical devices, such as bimorph, may avoid failure caused by interfacial debonding or stress concentration [3]. However, the commonly used piezoelectric materials are generally brittle in nature and have tendency to developing cracks during manufacturing and service processes. The existence of cracks may cause the constructive failure of the electromechanical systems. Moreover, these electromechanical systems made of piezoelectric materials are often being used or considered for using in the situations involving dynamic loading, thus the dynamic fracture analysis of FGPMs is of great importance in maintaining the mechanical integrity of these systems.

A critical issue involved in the fracture analysis of FGPMs is the electric boundary condition along crack surfaces. Most existing studies are limited to using electrically permeable [4] and impermeable [5] crack models. However, these two traditional models are not reasonable in some cases, according to some researchers [6-10]. As pointed out by Chiang and Weng [11], the dielectric permittivity of the crack medium will play a crucial role in Mode I crack. Therefore, it is essential to introducing the dielectric permittivity into the electric boundary conditions under tensile loading conditions. Considering dielectric medium effect, the fracture behaviour of homogeneous piezoelectric materials has been studied by some researchers [12-15]. Jiang [16] first attempted to use this dielectric crack model to investigate static problem of a crack in FGPMs.

In this work, we provide a theoretical study on the dynamic fracture behaviour of a propagating crack in FGPMs using dielectric crack model. The effect of

material gradient, crack propagating speed and dielectric medium inside the crack upon the dynamic fracture behaviour will be demonstrated. A critical state of the electromechanical loading applied to the medium is observed, which determines whether the traditional impermeable (or permeable) crack model serves as the upper or lower bound for the dielectric crack model. The methodology developed for the fracture analysis of FGPMs is also extended to study the problem of an interfacial crack between two dissimilar piezoelectric media, in which the interface is modeled as a layer with continuously varying material properties. Numerical simulations are given to show the effect of the interfacial layer parameters, such as, thickness of the interfacial layer and crack position upon the transition among different crack models.

2. Formulation and General Solutions of Crack in FGPMs

The problem envisaged is a plane strain problem of a finite crack moving at a constant speed V in an infinite functionally graded piezoelectric medium, which is subjected to external applied tensile stress σ_{22}^0 and electric displacement D_2^0. The original problem can be considered as a superposition of a uniform one and another one with crack surfaces subjected to electromechanical loading. Since the first one is trivial, we will focus on the second one as shown in Fig. 1a. The crack length is $2a$ and situates in the center, and there exists an electric potential drop across crack surfaces due to the crack deformation caused by applied loading. In addition to the fixed Cartesian coordinate system (x_1, x_2), a moving coordinate system (ξ_1, ξ_2) is attached to the crack center to describe the crack propagation.

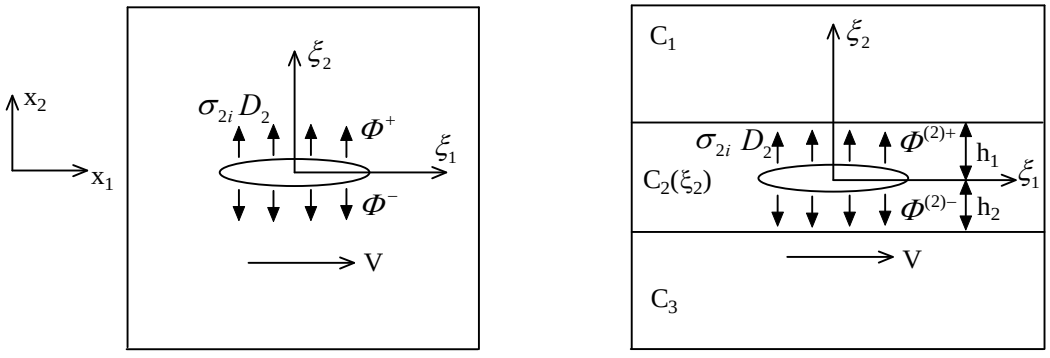

Fig. 1 Crack model

2.1 Governing equations

In the absence of body forces and free charges, the electromechanical behaviour of piezoelectric materials is governed by the equilibrium equations and Gauss law,

$$\sigma_{ij,j} = \rho \frac{\partial^2 u_i}{\partial t^2}, D_{i,i} = 0 \tag{1}$$

and the constitutive equations,

$$\sigma_{ij} = c_{ijrs}\varepsilon_{rs} - e_{rij}E_r, D_i = e_{irs}\varepsilon_{rs} + \epsilon_{ij}E_j \tag{2}$$

where $\mathbf{c}, \mathbf{e}, \boldsymbol{\epsilon}$ are elastic, piezoelectric and dielectric coefficients matrix, respectively. σ_{ij} and D_i are stress and electric displacement components, ϵ_{ij} and E_i are strains and electric field intensity defined as,

$$\varepsilon_{ij} = \frac{1}{2}(u_{i,j} + u_{j,i}), E_i = -\Phi_{,i} \tag{3}$$

with u_i and Φ being the displacements and electric potential.

The material constants $\mathbf{c}, \mathbf{e}, \boldsymbol{\epsilon}$ and the density of mass ρ may have arbitrary variation for FGPMs. However, to make the problem more mathematically tractable, it is assumed that they have the same exponential variation, for example,

$$\mathbf{c} = \mathbf{c}^0 e^{\alpha x_2}, \mathbf{e} = \mathbf{e}^0 e^{\alpha x_2}, \boldsymbol{\epsilon} = \boldsymbol{\epsilon}^0 e^{\alpha x_2}, \rho = \rho^0 e^{\alpha x_2} \tag{4}$$

where α represents the gradient of the material properties, $\mathbf{c}^0, \mathbf{e}^0, \boldsymbol{\epsilon}^0$ and ρ^0 are the material constants at the position of the crack line with,

$$\mathbf{c}^0 = \begin{bmatrix} c_{11}^0 & c_{12}^0 & 0 \\ c_{12}^0 & c_{22}^0 & 0 \\ 0 & 0 & c_{33}^0 \end{bmatrix}, \mathbf{e}^0 = \begin{bmatrix} 0 & e_{12}^0 \\ 0 & e_{22}^0 \\ e_{31}^0 & 0 \end{bmatrix}, \boldsymbol{\epsilon}^0 = \begin{bmatrix} \epsilon_{11}^0 & 0 \\ 0 & \epsilon_{22}^0 \end{bmatrix} \tag{5}$$

After introducing Galilean transformation,

$$\xi_1 = x_1 - Vt, \xi_2 = x_2 \tag{6}$$

the equations governing the electromechanical behaviour of FGPMs are derived as,

$$\frac{\partial^2 u}{\partial \xi_2^{\,2}} + \frac{c_{11}^0 - \rho^0 V^2}{c_{33}^0}\frac{\partial^2 u}{\partial \xi_1^{\,2}} + \frac{c_{12}^0 + c_{33}^0}{c_{33}^0}\frac{\partial^2 v}{\partial \xi_1 \partial \xi_2} + \frac{e_{12}^0 + e_{31}^0}{c_{33}^0}\frac{\partial^2 \Phi}{\partial \xi_1 \partial \xi_2} + \alpha\left(\frac{\partial u}{\partial \xi_2} + \frac{\partial v}{\partial \xi_1}\right) + \alpha\frac{e_{31}^0}{c_{33}^0}\frac{\partial \Phi}{\partial \xi_1} = 0 \tag{7}$$

$$\frac{\partial^2 v}{\partial \xi_2^{\,2}} + \frac{c_{33}^0 - \rho^0 V^2}{c_{22}^0}\frac{\partial^2 v}{\partial \xi_1^{\,2}} + \frac{c_{12}^0 + c_{33}^0}{c_{22}^0}\frac{\partial^2 u}{\partial \xi_1 \partial \xi_2} + \frac{e_{31}^0}{c_{22}^0}\frac{\partial^2 \Phi}{\partial \xi_1^{\,2}}$$

$$+ \frac{e_{22}^0}{c_{22}^0}\left(\frac{\partial^2 \Phi}{\partial \xi_2^{\,2}} + \alpha\frac{\partial \Phi}{\partial \xi_2}\right) + \alpha\frac{c_{12}^0}{c_{22}^0}\frac{\partial u}{\partial \xi_1} + \alpha\frac{\partial v}{\partial \xi_2} = 0 \tag{8}$$

$$\frac{\partial^2 \Phi}{\partial \xi_2^{\,2}} + \frac{\epsilon_{11}^0}{\epsilon_{22}^0}\frac{\partial^2 \Phi}{\partial \xi_1^{\,2}} - \frac{e_{31}^0}{\epsilon_{22}^0}\frac{\partial^2 v}{\partial \xi_1^{\,2}} - \frac{e_{22}^0}{\epsilon_{22}^0}\left(\frac{\partial^2 v}{\partial \xi_2^{\,2}} + \alpha\frac{\partial v}{\partial \xi_2}\right) - \frac{e_{12}^0 + e_{31}^0}{\epsilon_{22}^0}\frac{\partial^2 u}{\partial \xi_1 \partial \xi_2}$$

$$- \alpha\frac{e_{12}^0}{\epsilon_{22}^0}\frac{\partial u}{\partial \xi_1} + \alpha\frac{\partial \Phi}{\partial \xi_2} = 0 \tag{9}$$

2.2 Boundary Conditions

In this work, we only consider the cases where a tensile mechanical loading and an electric loading are applied to the piezoelectric medium. Under this situation,

the crack will open up and the dielectric medium will play a significant role in the fracture behaviour of FGPMs. Therefore, a dielectric crack model is used, the mechanical and electric boundary conditions along crack surfaces ($|\xi_1|<a$) are,

$$\sigma_{2i}^{+}=\sigma_{2i}^{-}=-\sigma_{2i}^{0}, D_2^{+}=D_2^{-}=-D_2^{e}, D_2^{e}=D_2^{0}+\epsilon_0\frac{\Phi^{+}-\Phi^{-}}{v^{+}-v^{-}} \tag{10}$$

where $\epsilon_0=8.85\times10^{-12}$CV/m is the dielectric permittivity of air (or vacuum) filling the crack. $v^{+}-v^{-}$ is the crack opening displacement caused by the applied loading. From Eq. (10), we may consider the effect of dielectric medium as introducing an extra electric displacement into the effective electric displacement D_2^{e} imposing on the crack surfaces, which is caused by the crack deformation. It indicates that this crack model is nonlinear and deformation-dependent. When $\epsilon_0=0$ or $\epsilon_0=\infty$, this model reduces to the traditionally impermeable and permeable crack models.

2.3 General Solutions

After using Fourier transform with respect to ξ_1, the general solutions of u^{*}, v^{*} and Φ^{*} satisfying the regularity conditions at infinity can be written as,

$$u^{*}(s,\xi_2)=\begin{cases}\sum_{i=1}^{3}C_{2i}e^{\lambda_{2i}\xi_2}, \xi_2>0\\ \sum_{i=1}^{3}C_{2i-1}e^{\lambda_{2i-1}\xi_2}, \xi_2<0\end{cases} \qquad v^{*}(s,\xi_2)=\begin{cases}\sum_{i=1}^{3}a_{2i}C_{2i}e^{\lambda_{2i}\xi_2}, \xi_2>0\\ \sum_{i=1}^{3}a_{2i-1}C_{2i-1}e^{\lambda_{2i-1}\xi_2}, \xi_2<0\end{cases}$$

$$\Phi^{*}(s,\xi_2)=\begin{cases}\sum_{i=1}^{3}b_{2i}C_{2i}e^{\lambda_{2i}\xi_2}, \xi_2>0\\ \sum_{i=1}^{3}b_{2i-1}C_{2i-1}e^{\lambda_{2i-1}\xi_2}, \xi_2<0\end{cases} \tag{11}$$

with * representing Fourier transform. C_i are unknown coefficients to be determined from boundary conditions, a_i and b_i are known coefficients in terms of λ_i and materials properties. λ_i are roots of the equation $\sum_{j=1}^{7}X_j\lambda^{7-j}=0$, relating to material properties and crack speed. Within the crack propagation speed range considered in this work, three of them $(\lambda_1,\lambda_3,\lambda_5)$ having positive real parts and the other three $(\lambda_2,\lambda_4,\lambda_6)$ having negative real parts.

As a mathematical model, a crack can be modeled as distributed dislocations. The generalized dislocation density functions are defined in terms of the jump of displacements and electric potential,

$$\psi_1(\xi_1)=\frac{\partial}{\partial\xi_1}\left[u(\xi_1,0^{+})-u(\xi_1,0^{-})\right], \qquad \psi_2(\xi_1)=\frac{\partial}{\partial\xi_1}\left[v(\xi_1,0^{+})-v(\xi_1,0^{-})\right],$$

$$\psi_3(\xi_1) = \frac{\partial}{\partial \xi_1}\left[\Phi(\xi_1, 0^+) - \Phi(\xi_1, 0^-)\right] \tag{12}$$

Then the stress and electric displacement field can be expressed in terms of the generalized dislocation density functions as,

$$\sigma_{2i}(\xi_1, 0) = \frac{1}{2\pi}\int_{-a}^{a}\sum_{j=1}^{3} K_{ij}(\xi_1, 0, \omega)\psi_j(\omega)\mathrm{d}\omega,$$

$$D_2(\xi_1, 0) = \frac{1}{2\pi}\int_{-a}^{a}\sum_{j=1}^{3} K_{3j}(\xi_1, 0, \omega)\psi_j(\omega)\mathrm{d}\omega \tag{13}$$

where $K_{ij}(\xi_1, 0, \omega) = \int_{-\infty}^{\infty} h_{ij}(s, 0)e^{-is(\omega-\xi_1)}\mathrm{d}s$ with h_{ij} being functions of s related to material properties and crack speed. The asymptotic analysis of h_{ij} indicates that these functions have the following properties,

$$\lim_{|s|\to\infty} h_{11}(s, 0) = iM_1\,\mathrm{sgn}(s), \lim_{|s|\to\infty} h_{22}(s, 0) = iM_2\,\mathrm{sgn}(s), \lim_{|s|\to\infty} h_{33}(s, 0) = iM_3\,\mathrm{sgn}(s)$$

$$\lim_{|s|\to\infty} h_{23}(s, 0) = iN_1\,\mathrm{sgn}(s), \lim_{|s|\to\infty} h_{32}(s, 0) = iN_2\,\mathrm{sgn}(s)$$

$$\lim_{|s|\to\infty} h_{12}(s, 0) = 0, \lim_{|s|\to\infty} h_{21}(s, 0) = 0, \lim_{|s|\to\infty} h_{13}(s, 0) = 0, \lim_{|s|\to\infty} h_{31}(s, 0) = 0 \tag{14}$$

Separating the singular parts of the kernels in Eq.(13) and substituting these equations into electromechanical boundary conditions (10) results in singular integral equations. These singular integral equations can be solved by expanding generalized dislocation density functions in terms of Chebyshev polynomials,

$$\psi_j(\omega) = \sum_{k=0}^{\infty} C_{jk}\frac{T_k(\omega/a)}{\sqrt{1-(\omega/a)^2}} \tag{15}$$

The resulting algebraic equations of electromechanical boundary conditions are numerically solved to determine the unknown C_{jk} by using collocation method. After C_{jk} are solved, the electromechanical fields of stress, electric displacement, displacement and electric potential are determined. Based on stress and electric displacement fields, fracture parameters, such as stress intensity factors K_I, K_{II}, electric displacement intensity factor K_D at the right tip of crack can be determined in terms of C_{jk}.

$$K_I(a) = -\sqrt{\pi a}(M_2\sum_{k=1}^{N} C_{2k} + N_1\sum_{k=1}^{N} C_{3k}),\ K_{II}(a) = -\sqrt{\pi a}M_1\sum_{k=1}^{N} C_{1k},$$

$$K_D(a) = -\sqrt{\pi a}(M_3\sum_{k=1}^{N} C_{3k} + N_2\sum_{k=1}^{N} C_{2k}) \tag{16}$$

From work of Dascalu [17], the dynamic energy release rate of cracked piezoelectric medium can be derived in terms of the stress and electric displacement intensity factors as,

$$G = \frac{1}{4}\left[\frac{K_{II}^2}{M_1} + \frac{K_I^2}{M_2} + \frac{N_1N_2K_I^2 + M_2^2K_D^2 - (N_1+N_2)M_2K_IK_D}{M_2(M_3M_2 - N_1N_2)}\right] \tag{17}$$

3. Interfacial Crack between Two Dissimilar Piezoelectric Media

The methodology developed in the previous section can be extended to study the interfacial crack between two dissimilar piezoelectric components as seen in Fig. 1b. To eliminate the oscillatory stress singularity at crack tips, the interface is modeled as a layer of piezoelectric medium with continuously varying material properties $C_2(x_2)$, which approach those of the upper plane $x_2 > h_1$ and lower plane $x_2 < -h_2$ as C_1 and C_3, respectively. The layer thickness is assumed as h, and the crack position is described by h_1 and h_2. Following the same procedure as in the previous section and using the continuity condition along bonded surfaces, the electromechanical fields for this interfacial crack problem can be derived to study the fracture behaviour. Within the crack speed range considered in this work, the treatment of interfacial layer model leads to the square root singularity in the stress and electric displacement fields at crack tips.

4. Results and Discussions

In numerical calculations, the material constants $\mathbf{c}^0, \mathbf{e}^0$ and $\boldsymbol{\epsilon}^0$ in Eq. (5) are taken as those of the PZT-4 ceramics for simulations. Firstly, we will pay attention to the effect of material gradient and crack speed upon the fracture behaviour when the medium is subjected to a tensile loading $\sigma_{22}^0 = 30\text{MPa}$ and an electric displacement $D_2^0 = 1\times10^{-3}\text{C/m}^2$. Fig. 2 shows the normalized stress intensity factor $k_I (k_I = K_I / K_I^0)$ versus materials gradient, where K_I^0 is the stress intensity factor calculated when material gradient $\alpha = 0$ and crack propagation speed $V = 0$. It can be seen that k_I increases with the increase of α for both static and dynamic cases. With the increase of V/c ($c = [(c_{22}^0 + (e_{22}^0)^2 / \epsilon_{22}^0) / \rho^0]^{1/2}$), k_I also increases, but $k_I = 1$ for homogeneous piezoelectric medium. This result is consistent with Yoffe's type crack in elastic materials. Due to the unsymmetry of material properties, there exists a coupling of crack opening mode and sliding model, which results in a nonvanishing K_{II}. Fig. 3 shows the effect of the material gradient on normalized stress intensity factor $k_{II} (k_{II} = K_{II} / K_I^0)$, it is observed that material gradient has a significant effect on k_{II} for both static and dynamic cases. For example, even for the static case $V/c = 0$, the normalized intensity factor k_{II} is about 0.26 when $\alpha a = 1$. It is obvious from this figure that the crack propagating speed will enhance the coupling between opening and sliding modes.

The effect of material gradient upon electric displacement intensity factor $k_D (k_D = K_D / K_D^0)$ is depicted in Fig 4, where K_D^0 is calculated when $\alpha = 0$ and $V = 0$. Similar phenomenon as in Fig 2 can be observed, however, $k_D \neq 1$ even for the dynamic problem of homogeneous piezoelectric medium. The variation of

the normalized dynamic energy release rate $g(g = G/G^0)$ versus material gradient is shown in Fig. 5, where G^0 is calculated when $\alpha = 0$ and $V = 0$. The material gradient effect on this parameter is obvious. From all these figures, we can see that all these fracture parameters change dramatically when crack speed is high, for example, $V/c = 0.4$, which may indicate the possible mode change at high crack speed.

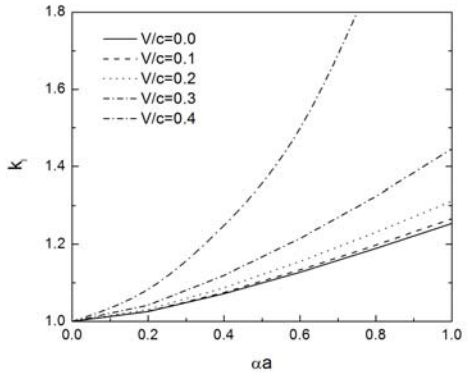

Fig. 2 Variation of the normalized k_I under electromechanical loading

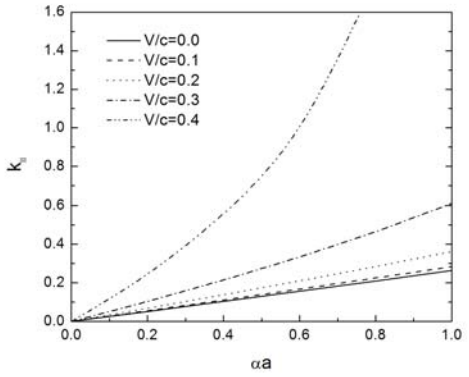

Fig. 3 Variation of the normalized k_{II} under electromechanical loading

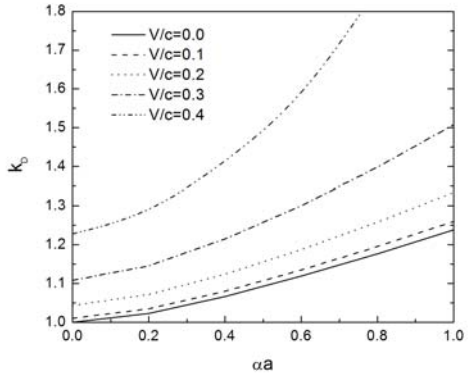

Fig. 4 Variation of the normalized k_D under electromechanical loading

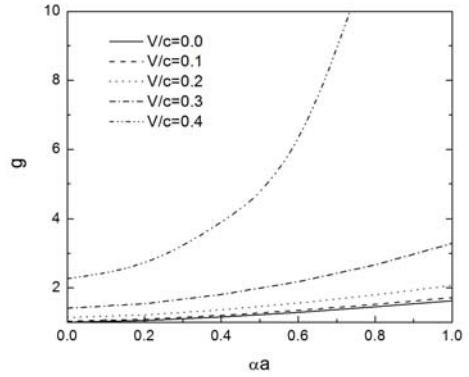

Fig.5 Variation of the normalized g under electromechanical loading

It is interesting to mention that the effect of dielectric medium inside the crack is the introduction of an extra term in effective electric displacement D_2^e as shown by Eq. (10). This effective electric displacement versus applied stress for different crack models is plotted in Fig. 6 with applied electric displacement $D_2^0 = 4\times10^{-3}\text{C/m}^2$ when $V/c = 0$ and $V/c = 0.2$ for both homogeneous ($\alpha a = 0$) and nonhomogeneous piezoelectric materials ($\alpha a = 0.4$ for example). Similar to the static problem in homogeneous cracked piezoelectric medium [11], there exists a critical state (σ_{22}^c, D_2^0) for applied electromechanical loading. For fixed

applied electric loading D_2^0, when the applied stress $\sigma_{22}^0 < \sigma_{22}^c$, the response of an impermeable and permeable cracks serves as the upper and lower bound respectively. However, when $\sigma_{22}^0 > \sigma_{22}^c$, the situation is completely reversed. It demonstrates in this figure that this critical state for electromechanical loading will change with crack speed and material gradient.

To see if there exists such a critical value for σ_{22}^c for the interface crack in two dissimilar piezoelectric materials, the variation of effective electric displacement D_2^e with applied tensile stress σ_{22}^0 under applied electric displacement $D_2^0 = 5\times10^{-3}\text{C/m}^2$ is plotted in Fig. 7. In this case, the material constants for lower piezoelectric medium are taken as those of the PZT-4 ceramics and material mismatch is set to be $C_3/C_1 = 1/5$. It demonstrates from this figure that there does exist such a critical value σ_{22}^c, and the interfacial layer model parameters, such as interfacial layer thickness and crack position (h_1/h), has a significant effect upon this critical state for electromechanical loading. From Fig. 6 and Fig. 7, we can see that the results for the dielectric crack model are always between traditionally impermeable and permeable crack models. Therefore, this dielectric crack model might be more accurate to predict the dynamic fracture behaviour of cracked FGPMs for some cases. The transition among different crack models is obvious depending on the applied electromechanical loadings.

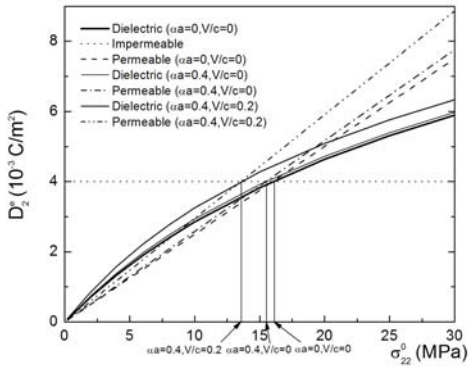

Fig.6 Variation of effective electric displacement with the applied stress for different models

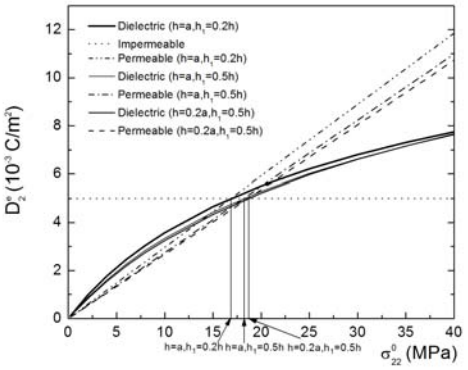

Fig.7 Variation of effective electric displacement with the applied stress for interface crack

5. Conclusion

This work provides a theoretical study on a finite moving crack in FGPMs subjected to inplane electromechanical loading. Numerical results show that the material gradient and crack speed have great influence on the fracture behaviour of cracked FGPMs. Investigation on the effect of dielectric medium filling the crack upon the dynamic fracture behaviour of FGPMs indicates that dielectric crack model may be more accurate for the fracture analysis of FGPMs. A critical state of electromechanical loading exists, which determines whether the

impermeable and permeable models serve as the upper or lower bound of the dielectric crack model. This critical state is affected by the crack speed and material gradient and can only be calculated numerically. The fracture behaviour of interfacial crack problem has also been investigated by using an interfacial layer model. Numerical calculations indicate that the parameters of this layer model have significant effect on the transition among different crack models.

Acknowledgement

This work was supported by the Natural Sciences and Engineering Research Council of Canada (NSERC).

References

[1] K.S. Ravichandran, Thermal residual stresses in a functionally graded material system, Mat Sci Eng A-Struct 201(1/2) (1995) 269-276
[2] Y. Obata, N. Noda, Steady thermal stresses in a hollow circular cylinder and a hollow sphere of a functionally gradient material, J Therm Stress 17(3) (1994) 471-487
[3] K.Takagi, J.F.Li, S. Yokoyama, R. Watanabe, A. Almajid, M. Taya, Design and fabrication of functionally graded PZT/Pt piezoelectric bimorph actuator, Sci Technol Adv Mater 3(2) (2002) 217-224
[4] V.Z. Parton, Fracture mechanics of piezoelectric materials, Acta Astronaut 3(9/10) (1976) 671-683
[5] W.F.J. Deeg, The analysis of dislocation, crack and inclusion problems in piezoelectric solids, PhD thesis, Stanford University, 1980
[6] R.M. McMeeking, Electrostrictive stresses near crack-like flaw, Z Angew Math Phys 40(5) (1989) 615-627
[7] H. Sosa, Plane problems in piezoelectric media with defects, Int J Solid Struct 28(4) (1991) 491-505
[8] M.L. Dunn, The effects of crack face boundary conditions on the fracture mechanics of piezoelectric solids, Eng Fract Mech 48(1) (1994) 25-39
[9] T.Y. Zhang, P. Tong, Fracture mechanics for a mode III crack in a piezoelectric material, Int J Solid Struct 33(3) (1996) 343-359
[10] T.Y. Zhang, C.F. Qian, P. Tong, Linear electro-elastic analysis of a cavity or a crack in a piezoelectric material, Int J Solid Struct 35(17) (1998) (2121-2149)
[11] C.R. Chiang, G.J. Weng, Nonlinear behaviour and critical state of a penny-shaped dielectric crack in a piezoelectric solid, J Appl Mech-T ASME 74(5) (2007) 852-860
[12] T.H. Hao, Z.Y. Shen, A new electric boundary condition of electric fracture mechanics and its applications, Eng Fract Mech 46(6) (1994) 793-802
[13] X.L. Xu, R.K.N.D Rajapakse, On a plane crack in piezoelectric solids, Int J Solids Struct 38(42/43) (2001) 7643-7658
[14] X.D. Wang, L. Y. Jiang, Fracture behaviour of cracks in piezoelectric media with electromechanically coupled boundary conditions, Proc R Soc London A 458(2026) (2002) 2545-2560

[15] X.D. Wang, L. Y. Jiang, The nonlinear behaviour of an arbitrarily oriented dielectric crack in piezoelectric materials, Acta Mech 172(3/4) (2004) 195-210
[16] L.Y. Jiang, The fracture behaviour of functionally graded piezoelectric materials with dielectric cracks, Int J Fracture 149(1) (2008) 87-104
[17] C. Dascalu, G.A. Maugin, On the dynamic fracture of piezoelectric materials, Q J Mech Appl Math 48 (1995) 237-255